Theoretical and Applied Climatology
https://doi.org/10.1007/s00704-024-04898-7

RESEARCH

Predictability of the atmospheric circulation patterns in Africa, south of the equator, using variations of the Southern Annular Mode and ENSO

Chibuike Chiedozie Ibebuchi[1,2]

Received: 12 July 2022 / Accepted: 22 February 2024

Abstract
The contribution of the El Niño Southern Oscillation (ENSO) and the Southern Annular Mode (SAM) to the variations of the leading modes of atmospheric circulation in Africa south of the equator, during austral summer (i.e., from December to March), is examined in this study. The rotated principal component analysis is applied to classify the leading modes of atmospheric circulation in the study region. The result showed that relatively, through the control of sea level pressure in the mid-latitudes, the SAM is more related to the variability of the austral summer leading modes of atmospheric circulation in the study region. Overall, during the analysis period, the SAM explained about 20% to 46% variance of the leading atmospheric circulation modes. ENSO rather explains up to about 10% to 20% of the variance. Due to the continuous nature of atmospheric circulation, incorporating the co-variability of the classified circulation patterns adds skill to the predictability of the classified leading modes. Overall, the joint variations of the SAM, ENSO, and other less frequent regional circulation patterns that are related to classified leading modes, explained up to 46% to 80% variance of the leading modes—which is indeed an added value in further considering the natural gradient of the classified circulation patterns.

1 Introduction

The synoptic patterns of atmospheric circulation at a given time loosely correspond to atmospheric signals with time scales of daily, inter-annual, decadal variations, and climate change (Compagnucci et al. 2001). Also, the continuum nature of atmospheric processes implies that at a given instant, the signals of different patterns of atmospheric circulation interact. According to Huth et al. (2008), teleconnections are the building blocks of atmospheric circulation patterns. Thus, the inter-annual to decadal variability of teleconnections can impact the behavior of circulation patterns at a given region and time (Pohl et al. 2018). Among the climate drivers that can influence the regional climate of southern Africa, the Southern Annular Mode (SAM) and the El Niño Southern Oscillation (ENSO) are two established climate drivers that can significantly impact the regional hydroclimate of southern Africa (e.g. Reason et al. 2000; Hoell et al. 2015; Hart et al. 2018; Ibebuchi 2021a, c; Ibebuchi and Lee 2024). This study examines the relative contributions of ENSO and SAM in explaining the variations of the leading modes of atmospheric circulation in Africa south of the equator, during austral summer (i.e., from December to March: DJFM).

The SAM is associated with anomalous low (high) sea level pressure (SLP) at the southern hemisphere mid-latitudes during its negative (positive) phase (Thompson and Wallace 2000). Variations of the SAM can impact ocean circulation (Hall and Visbeck 2002), sea surface temperature variability (Screen et al. 2009), and regional modes of atmospheric circulation in southern Africa (Engelbrecht and Landman 2016; Ibebuchi 2021a). According to Thompson and Wallace (2000), the SAM can explain about 20%—30% variance of the total monthly SLP variability south of 20°S. ENSO on the other hand is associated with tropical Pacific Sea surface temperature anomalies. During ENSO's positive (negative) phase, sea surface temperature in the central and eastern tropical Pacific Ocean is warmer (cooler) than normal. Compared to the SAM, ENSO has rather a remote influence on the regional modes of atmospheric circulation in southern Africa (Reason and Jagadheesha 2005). Cook

✉ Chibuike Chiedozie Ibebuchi
cibebuch@kent.edu

[1] Department of Geography, Kent State University, Kent, OH, USA

[2] ClimRISE Lab, Kent State University, Kent, OH, USA

Published online: 04 March 2024

(2000) reported that El Niño impacts the regional climate of southern Africa by weakening the Mascarene high and the Angola low which both principally contribute to the strength and position of the South Indian Ocean Convergence Zone (Pohl et al. 2009). Hoell et al. (2015) noted that because of the moderations in convection in the tropical Indian Ocean and the Pacific Ocean by the ESNO signal, Rossby waves are induced over southern Africa, which modulates southeasterly moisture fluxes and vertical motion over southern Africa landmasses. Ibebuchi (2021c) linked ENSO events to anomalies in regional circulation types (CTs) in southern Africa; the author found that El Niño through the deepening of cyclonic activity in the southwest Indian Ocean weakens the western branch of the Mascarene high and disrupts southeasterly moisture fluxes from the southwest Indian Ocean. As a result, El Niño tends to increase (decrease) the amplitude and frequency of occurrence of leading atmospheric circulation patterns associated with westerly (southeasterly) fluxes of moisture across the southwest Indian Ocean.

Atmospheric processes have a fuzzy physical nature. SAM and ENSO are not orthogonal likewise. L'Heureux and Thompson (2006) found that during austral summer, up to 25% of the variance of the SAM can be related to ENSO variations. Ding et al. (2012) noted that the SAM index reflects the superposition of both high-latitude and tropically forced variability. Several studies have addressed the role of climate drivers in modulating atmospheric circulations in southern Africa (Cook 2000; Reason et al. 2006; Dieppois et al. 2016; Engelbrecht and Landman 2016; Pohl et al. 2018; Ibebuchi 2021a). However, a time decomposition of the atmospheric circulation patterns (containing all time scales) in southern Africa; the relative contribution of climate drivers to the variations in the circulation patterns, and the value-added by the natural gradient in the circulation patterns in improving their predictive skill has not been addressed, at least from the aspect of the fuzzy nature of atmospheric circulations. Previous studies (e.g., Ibebuchi 2021a) used the T-mode (i.e., the variable is time series and observation is grid points) obliquely rotated principal component analysis (PCA) technique (Richman 1981; Richman. 1986; Philipp 2009; Ibebuchi and Richman 2023) to classify CTs in Africa south of the equator. According to Compagnucci et al. (2001), the time decomposition with the rotated T-mode PCA results in CTs that contain all time scales ranging from daily synoptic developments, low-frequency variability, climate fluctuations, and change. Hence the rotated T-mode PCA classification method suits the purpose of this study since analyzing the relationship between the classified CTs and climate drivers is crucial. Therefore, this study uses the already classified CTs from previous works, to examine how ENSO and SAM explain variations of the classified leading circulation modes during austral summer. Also, to what extent the anomalies in the leading circulation modes during austral summer can be predicted using their teleconnections and the natural gradient arising from the circulation patterns will be investigated.

2 Data and methodology

SLP, 850 hPa wind vector, and specific humidity data set are obtained from ERA5 (Hersbach et al. 2020) and NCEP-NCAR (Kalnay et al. 1996) for the 1979–2020 period. The temporal resolution is daily. The horizontal resolution for the ERA5 data set is 0.25° longitude and latitude, and 2.5° longitude and latitude for the NCEP-NCAR data set.

This work is an extension of previous studies (Ibebuchi 2021a, c) that applied obliquely rotated T-mode PCA time decomposition technique to classify CTs that contain the three aspects of time scale variability, i.e. high-frequency variability, low-frequency variability, and variations due to anthropogenic influence (Compagnucci et al. 2001) in Africa south of the equator. Thus, the methods for the CT classification and the resultant CTs are also the same. The explanation of the method is presented in the Appendix section. However, unlike the previous studies, the focus in this present work will be on the predictability of the leading modes. Since the rotated PCA classification results in a solution with a large number of dimensions; the "leading circulation modes" are defined as the first PC loading patterns that have a congruence match of ≥ 0.92 (i.e., the range required to ensure minimum noise to signal ratio in the PC loading patterns according to Ibebuchi and Richman 2023) with correlation vector that they are indexed to. The modulation of the SAM and ENSO over the occurrence of leading circulation modes during austral summer (December to March), when the relationship between southern African rainfall and ENSO is strongest (Manatsa et al. 2015) is examined.

The relationship between anomalies in large-scale climate drivers and the leading circulation modes in the study region can have a persistent impact on the overall mean state of the atmosphere in the study region (e.g., Dieppois et al. 2016). Nevertheless, the signals in other relatively rare CTs might also impact the mean state of the leading CTs. Thus, using correlation analysis and linear regression analysis, the relationship over time, between the leading circulation modes, the SAM index, Niño 3.4 index, and other relatively rare CTs is investigated. The SAM index is obtained from https://climatedataguide.ucar.edu/climate-data/marshall-southern-annular-mode-sam-index-station-based. The Niño 3.4 index is obtained from https://psl.noaa.gov/gcos_wgsp/Timeseries/Nino34/. Both indices are obtained for the 1979–2020 period. Unlike Ibebuchi (2021c) which considered all-season correlations between ENSO and the CTs, the point correlation analysis in this work is exclusively focused on the DJFM season.

The non-parametric and resistant Kendall Tau-b test is used to test for the statistical significance of the correlation at a 95% confidence level. For the linear regression analysis, non-parametric bootstrapping at a 95% confidence level (based on 1000 replications) is used for the R-squared (i.e., percentage of variance explained). It should be noted that a significant correlation implies a rough estimate of the modulation in time of the teleconnection over the occurrence and amplitude of the CT.

Finally, the predictive skill of the covariates (i.e., ENSO, SAM, and the gradient of other less frequent CT) on the anomalies in the leading circulation modes are examined using stepwise linear regression to determine the best fit and then multiple linear regression analysis. The training period when the regression coefficients are obtained is from 1979 to 1999. The coefficients are then used in predicting the DJFM temporal variability of the amplitude of the leading circulation modes during the 2000 to 2020 test period.

3 Results and discussion

Appendix Figs. 5 and 6 show the CTs classified from the previous studies, and their probability of occurrence, respectively, as obtained when the classification scheme is independently applied to the ERA5 and NCEP SLP data. The probabilities of occurrence of the CTs do not add up to 100% since a day can be assigned to more than one CTs, i.e., the CTs that occurred on the day in question. CTK + and CTK − indicate circulation types derived from the positive phase and negative phase, respectively, of the Kth retained principal component loadings. For example, CT1 + and CT1 −, are the CTs obtained from the positive phase and negative phase of *PC1*, henceforth referred to as *Type 1*—to designate the mode of variability captured by PC1 (i.e., considering both its positive and negative phase).

CT1 +, CT2 −, and CT3 + are relatively the most frequent CTs (Appendix Fig. 6). Accordingly, Type 1 (CT1 +/CT1 −), Type 2 (CT2 +/CT2 −), and Type 3 (CT3 +/CT3 −) have the largest congruence matches with the correlation vectors they are indexed to, implying maximum signal-to-noise ratio. Thus, Type 1, Type 2, and Type 3 are relatively the dominant CTs in the study region (i.e., they are designated as the leading circulation modes in this study).

Figure 1 additionally shows the composite of 850 hPa moisture flux for the selected CTs (from the leading circulation modes). In CT1 +, the mid-latitude cyclone tracks slightly northward, and the semi-permanent subtropical anticyclone equally shifts north over the southern African region. The inverse phase of Type 1 (i.e., CT1 −) shows a synoptic state that is rather not favorable for the occurrence of CT1 +. In CT1 − it can be seen that the South Atlantic anticyclone shifts southward, blocking the mid-latitude cyclone from tracking further north (Fig. 1). Consequently, CT1 + (CT1 −) can be associated with westerly (southeasterly) moisture fluxes across large parts of South Africa and Agulhas current (Fig. 1). From Table 1, Type 1 is negatively correlated with the SAM index and positively correlated with the Niño 3.4 index. This implies that during DJFM, CT1 + is related to negative SAM and the above-average Niño 3.4 index (El Niño). On the other hand, CT1 − is related to the positive SAM index and below-average Niño 3.4 index (La Niña). The physical justification of the relationship is that during El Niño/negative SAM (La Niña/positive SAM) westerly (southeasterly) winds are enhanced over southern Africa (e.g., Jury 2015). Moreover, during the analysis period, a significant correlation (R= − 0.28) was found between the SAM index and the Niño 3.4 index. Thus, El Niño can be related to negative SAM and vice versa (L'Heureux and Thompson 2006). The relationship between Type 1 and SAM is relatively higher (Table 1). From Table 2, the result of the linear regression indicates that during DJFM, the SAM explains up to about 25% variance of Type 1 while ENSO explains about 12%. These results are in line with studies (e.g., Mason and Jury 1997; Rouault and Richard 2005; Pohl et al. 2009; Dieppois et al. 2015) on the control of synoptic circulations in southern Africa by the anomalies of ENSO and the SAM.

Type 2 presents the circulation modes of variability at the western branch of the Mascarene high (Fig. 1). In CT2 +, the anticyclonic circulation at the western branch of the Mascarene high is stronger and positions southward deforming the mid-latitude cyclone to track/strengthen equatorward, south of the western parts of South Africa. Thus, there is the inference of southeasterly fluxes driven by the Mascarene high and westerly fluxes driven by the mid-latitude cyclones (Fig. 1). CT2 − shows a weaker and more eastward state of the western branch of the Mascarene high compared to CT1 +. Resultantly, westerly moisture fluxes dominate over the mid-latitudes and the southwest Indian Ocean (Fig. 1). From the ERA5 data, Type 2 was found to be positively correlated with the SAM (Table 1). Based on the linear regression analysis, the SAM explains about 13% variance of Type 2. While the relationship cannot be externally validated using the NCEP data, the significant relationship from ERA5 might be physically interpreted, but with caution. The positive correlation between SAM and Type 2, implies that CT2 + is related to positive SAM. According to Xue et al. (2003), during positive SAM when SLP increases in the mid-latitudes, stronger anti-cyclonic circulation at the Mascarene high can be expected. CT2 − is related to negative SAM, and similar to CT1 +, enhanced westerly over the mid-latitudes is evident (Fig. 1).

From Table 1, Type 3 is more related to the SAM and ENSO compared to Type 1 and Type 2. The relationship between Type 3 and the SAM is however stronger compared to ENSO. From Table 2, up to 46% variance in Type 3 can be explained by variations of the SAM during DJFM. ENSO

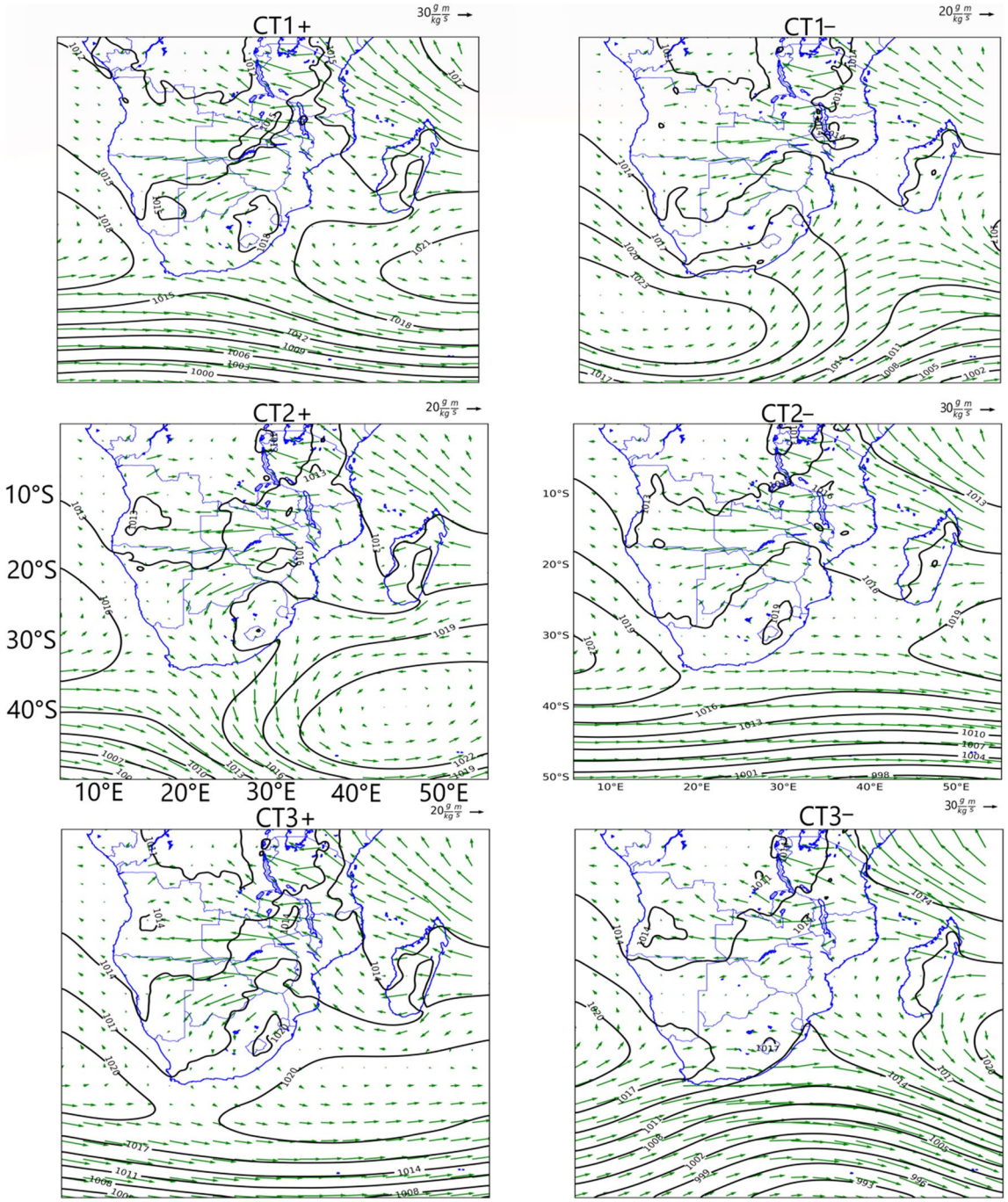

Fig. 1 SLP composite (black contours) and moisture flux composite (green vectors) of the leading circulation modes in Africa South of the equator

explains about 20%. The negative correlation between Type 3 with the Niño 3.4 index and the positive correlation with the SAM index (Table 1) implies that CT3 + (CT3 −) is related to La Niña/positive SAM (El Niño/negative SAM). Due to the relatively stronger relationship between Type 3 and SAM, Fig. 1 shows that the high (low) SLP, coupled with a suppressed (enhanced) band of westerly at the mid-latitudes that features during positive (negative) SAM are well expressed in Type 3. Overall, the SAM is relatively more related to the leading circulation modes and explains more of their DJFM variance compared to ENSO. The signal of the SAM and ENSO on the leading modes is expressed mainly through variations in the strength and zonal/meridional positioning of the subtropical anticyclones.

Table 1 Kendall's correlation coefficient between the DJFM climate indices and the dominant modes during the 1979–2020 period

	ERA5	NCEP
Type 1		
SAM	−0.33	−0.38
Niño 3.4	0.22	0.27
Type 2		
SAM	0.23	0.16*
Niño 3.4	−0.04*	−0.05*
Type 3		
SAM	0.49	0.39
Niño 3.4	−0.26	−0.23

Correlations that are not statistically significant at a 95% confidence level based on the Kendall Tau-b test are marked by an asterisk (*)

Table 2 Percentage of variance in the dominant modes explained by the variations of SAM and Niño 3.4 index, using linear regression, during DJFM for the 1979–2020 period

	ERA5	NCEP
Type 1		
SAM	0.20 [0.02, 0.44]	0.25 [0.04, 0.49]
Niño 3.4	0.10 [0.00, 0.30]	0.12 [0.01, 0.36]
Type 2		
SAM	0.13 [0.00,0.32]	–
Niño 3.4	–	–
Type 3		
SAM	0.46 [0.26, 0.62]	0.34 [0.11,0.53]
Niño 3.4	0.20 [0.02,0.44]	0.17 [0.01,0.42]

Dash (-) indicates correlations from Table 1 that are not statistically significant. The 95% confidence interval of the R-squared is written in the parenthesis

Given that both reanalysis data sets agree on a stronger significant relationship between Type 1, Type 3, and the SAM, Fig. 2 shows the time series of Type 1, Type 3, and the SAM index from 1979 to 2020. The first four strongest DJF El Niño and La Niña years since 1979 are used as the benchmark to investigate if the ENSO signal modulates the relationship between SAM and the leading circulation modes. 1983 and 1992 are two strong El Niño years that were accompanied by significant drought episodes (Mason and Tyson 2000; Ibebuchi 2021c). Figure 2 (top panel) suggests that during 1983 and 1992, the strong El Niño event, coupled with a significantly below-average SAM index might have amplified the gradient between SAM and Type 1 (i.e. an anomalous increase (decrease) in the amplitude of CT1 + (CT1 −)). Also, from Fig. 2 (bottom panel) Type 3 is below-average (i.e. increase (decrease) in the amplitude of CT3 − (CT3 +)). During the 1998 El Niño event, the projected drought in southern Africa failed to materialize (Lyon and Manson 2007). During 1998, the SAM was positive (Fig. 2). Hence unlike in 1992 and 1983, during 1998 the amplitude of CT3 +, which is a wet pattern was not constrained (Fig. 2, bottom panel). A similar argument can be inferred from other years highlighted in Fig. 2—for example, during the 2008 and 2011 La Niña events. Overall, when ENSO and SAM are significantly out of phase (i.e. negative SAM and El Niño, or positive SAM and La Niña), there is the likelihood that their joint impact on the regional circulation modes will be amplified. On the other hand, when ENSO and SAM are in the same phase (i.e. negative SAM and La Niña, or positive SAM and El Niño), there is the likelihood that their joint impact on regional circulation modes will be buffered. This can be related to the fact that during austral summer, El Niño is related to negative SAM and vice versa (e.g., Seager et al. 2003).

Next, given that atmospheric circulation at a given time is not discrete but continuous, it is examined how the gradient of the classified CTs in Appendix Fig. 5 modulates the spatiotemporal variability of the leading circulation modes. Table 3 shows the DJFM statistical correlations over time between the classified CTs in Appendix Fig. 5. Interestingly, some of the CTs are significantly correlated during DJFM. More focus will be placed on Type 1, Type 2, and Type 3 (i.e., the leading circulation modes). First, from Table 3, Type 1 is negatively correlated with Type 3. This implies that CT1 + is related to CT3 −, and CT1 − is related to CT3 +. Thus, an increase in the amplitude of CT1 + will tend to decrease the amplitude of CT3 + and vice versa, which is typically what might be expected during ENSO events as reported in Ibebuchi (2021c). Physically, the relationship between CT1 + and CT3 − can be inferred from Appendix Fig. 5. CT3 − is an extreme case of CT1 + based on the strengthening and northward track of the mid-latitude cyclones, which can further weaken and disintegrate the subtropical ridges over South Africa and beyond. Thus, the positive correlation over time of both CTs suggests that both CTs are dynamically linked. From Table 1, CT1 + is also positively correlated to CT5 −, CT7 + and CT8 + and vice versa for CT1 −. CT5 −, CT7 + and CT8 + all feature a weaker western branch of the Mascarene high, similar to CT3 −, and enhanced cyclonic activity in the southwest Indian Ocean (c.f. Appendix Fig. 5). The result suggests that the weakening of the western branch of the Mascarene high, strengthening and northward track of the mid-latitude cyclones, and enhanced cyclonic activity in the southwest Indian Ocean are fuzzy/continuous atmospheric processes that can be interrelated. According to Morioka et al. (2015), positive sea surface temperature anomalies (i.e., enhanced cyclonic activity) in southwest Indian tend to weaken the Mascarene high. Also, Xue et al. (2003) noted that during negative SAM when the mid-latitude cyclone tends to track northward and strengthen at the mid-latitudes, the weakening of the Mascarene high can be expected. As highlighted

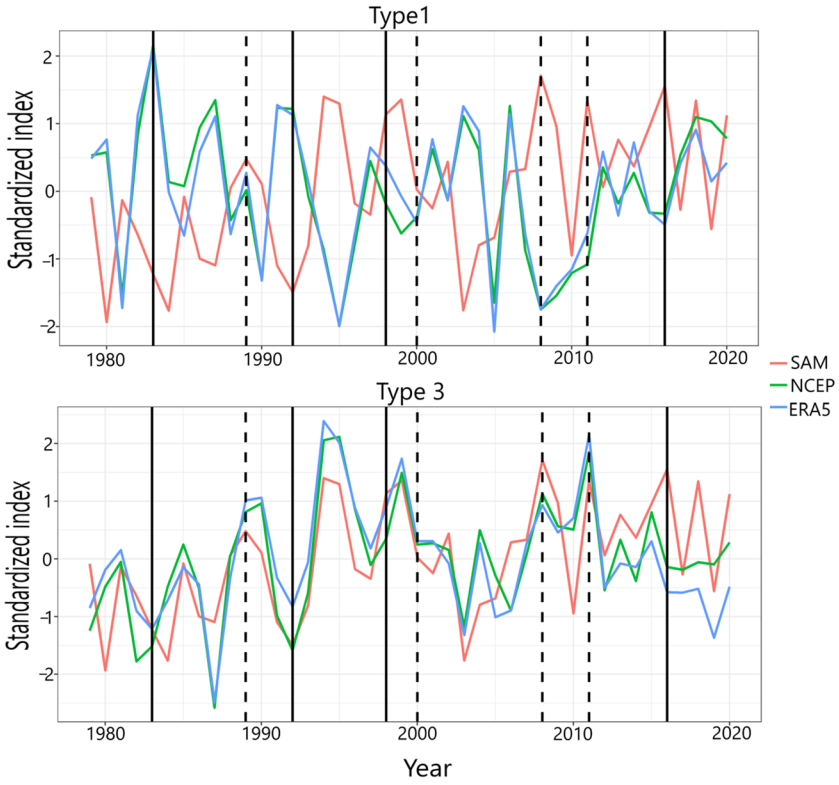

Fig. 2 December-March time series of the Southern Annular Mode index and the loadings of Type 1 and Type 3 from ERA5 and NCEP for the 1979–2020 period. The vertical dotted (thick) lines highlight the first four years with strong La Niña (El Niño) during DJF since 1979. The strong El Niño years are 1983, 1992, 1998, and 2016. The strong La Niña years are 1989, 2000, 2008 and 2011. The first four strong ENSO years since 1979 are based on the categorizations from https://psl.noaa.gov/enso/climaterisks/years/top24enso.html

Table 3 Correlation coefficient between the classified patterns during DJFM for the 1979–2020 period

	Type1	Type2	Type3	Type4	Type5	Type6	Type7	Type8	Type9
Type1			− 0.66	–	− 0.51	–	0.49	− 0.47	–
Type2			0.61	− 0.38	–	–	–	–	–
Type3	− 0.66	0.61		− 0.44	0.40	–	− 0.39	–	–
Type4		− 0.38	− 0.43	–	–	–	− 0.35	–	–
Type5	− 0.51	–	0.40	–	–	− 0.37	–	–	–
Type6	–	–	–	–	− 0.37	–	–	–	–
Type7	0.49	–	− 0.39	− 0.35	0.28	–	–	–	–
Type8	− 0.47	–	–		–	–	–	–	–
Type9			–	− 0.23	–	–	–	–	–

Correlations that are not statistically significant at a 95% confidence level based on the Kendall Tau-b test are not reported. Dash (-) indicates correlations that are not statistically significant

by Morioka et al. (2015), the northward shift of the storm tracks (and the westerly jet) favors the weakening of the Mascarene high in its southern part. Thus, the prediction of the behavior of Type 1 over time can benefit from incorporating the aforementioned fuzzy physical processes.

Furthermore, atmospheric conditions that favor the strengthening of the Mascarene high can be inferred from reverse mechanisms that are asymmetric. From Table 3, CT3 +, which favors strengthening of the Mascarene high, is related to CT1 −, CT2 +, CT4 +, CT5 +, and CT7 − during DJFM. Appendix Fig. 5 shows that the aforementioned CTs tend to favor atmospheric blocking of the mid-latitude cyclone by the subtropical anticyclones, south of Madagascar and/or south of South Africa; overall, favoring the synoptic state of CT3 +. Interestingly, CT6 − presents a synoptic state associated with stronger circulation at the western branch of the Mascarene high. Table 3 shows that CT5 + is related to CT6 −. Thus, an increase in the amplitude of CT5 + can imply a strengthening of the western branch of the Mascarene high under CT6 −. CT5 + is related to the La Niña signal (Ibebuchi 2021c) that enhances anti-cyclonic circulation at the Mascarene high (Cook 2000; Hart et al. 2018). Thus, during austral summer, the increase in the amplitude of CT3 +, triggering an increase in the amplitude of CT5 + implies also an increase in the amplitude of CT6 −. On the other hand, Appendix Fig. 5 shows that CT5 − is

associated with enhanced cyclonic activity in the southwest Indian Ocean thus increasing its amplitude can weaken the Mascarene high. The natural gradient arising from a fuzzy set of circulation patterns can help understand further the physics governing the evolution of the classified CTs and the feedback atmospheric process associated with the continuum atmospheric system.

Using multiple linear regressions, Fig. 3 shows the predictions of the inter-annual fluctuations of the amplitude of Type 3 using the SAM and ENSO (Fig. 3a) alone; and adding equally the gradient of other Types (as contained in Table 3) that covary with Type 3 (Fig. 3b). It can be seen (also from Table 4) that there can be a relative improvement in the predicted values when both the teleconnections related to Type 3 and other Types that covary with Type 3 are considered. Resultantly up to 80% variance in Type 3 can be explained (Table 4). Similarly, the same result holds for Type 1 and Type 2 (Fig. 4 and Table 4). The prediction in the amplitudes of the leading circulation modes is relatively more accurate for Type 3, given its stronger relationship with the SAM. Type 3 can be a good predictor for other leading circulation modes (Table 3). Thus, while there might not be a direct correlation between ENSO, SAM, and some CTs, the gradient/fuzzy nature of the atmospheric processes allows further interpretation of how the circulation modes related to ENSO and the SAM can modulate other CTs that are not directly related to the teleconnections. Hence an indirect relationship can be established so that the predictability of any given circulation mode might be enhanced.

Table 4 Explained variance of the dominant modes by the teleconnections and other Types they covary with them during DJFM for the 1979–2020 period

Type	ENSO and SAM	All covariates
Type 1	0.24 [0.03, 0.48]	0.69 [0.56, 0.76]
Type 2	0.17 [0.01, 0.38]	0.46 [0.18, 0.60]
Type 3	0.53 [0.29, 0.66]	0.80 [0.66, 0.85]

The 95% confidence interval of the R-squared is written in the parenthesis

Given that when the classification scheme used in this paper has been successfully applied to appropriate global climate models, the CTs can be externally validated as observed, even under different climatic conditions (e.g., Ibebuchi 2021a, b). A further implication of this study is that it can help modelers develop the capability of climate models to simulate the large-scale patterns of atmospheric circulation in a given region. This is because the co-variability between a given CT signal and other signals is established. Thus, when a climate model underperforms in simulating a

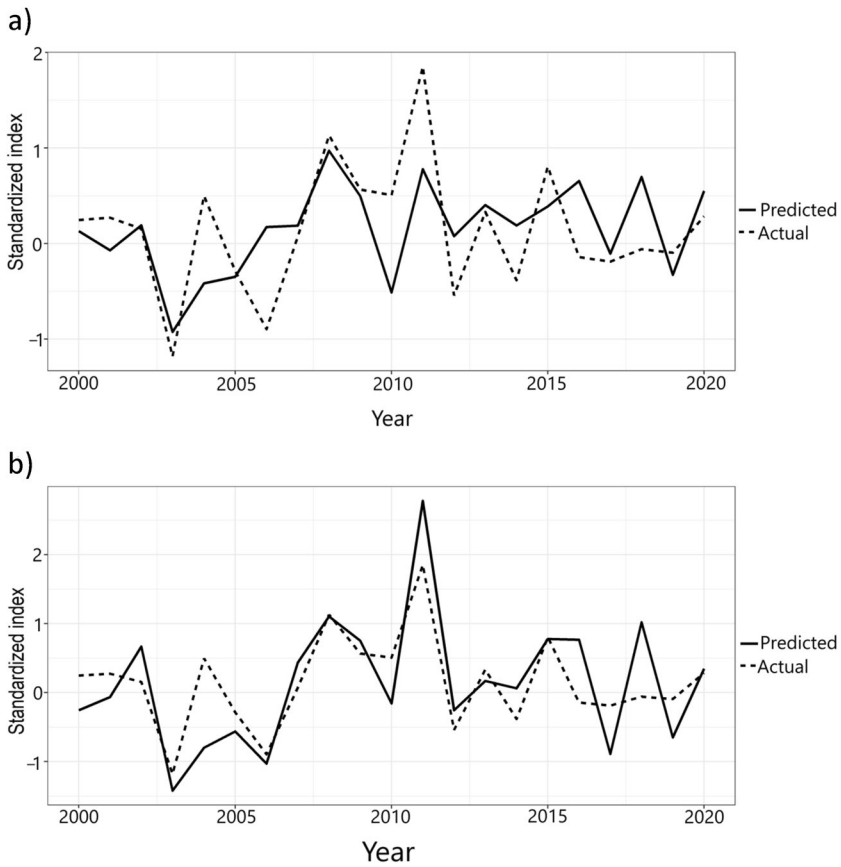

Fig. 3 Predicted and actual values of the loadings (amplitude) of Type 3 using the SAM and Niño 3.4 index (**A**) and the SAM, Niño 3.4 index, and the loadings of other modes related to Type 3 (**B**). For the multiple linear regression analysis, the training period when the regression coefficients are obtained is 1979 to 1999. The coefficients are used in predicting the DJFM fluctuations in the amplitude of the mode during the validation period from 2000 to 2020

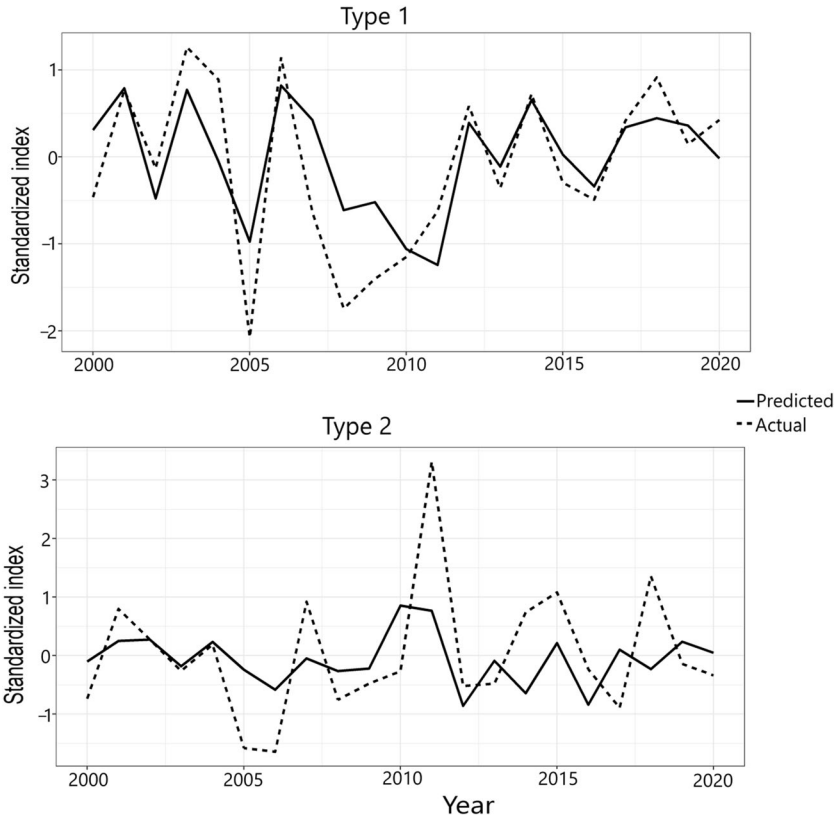

Fig. 4 Same as Fig. 3b but for Type 1 and Type 2

given CT, it can be deduced how other CTs can be affected or a targeted correction (in the course of model development) can be made on the synoptic circulations.

Finally, considering the decadal fluctuations in summer southern African rainfall (e.g., Malherbe et al. 2014) this study contributes to the existing literature by also showing how the CTs derived from the simple method of fuzzy obliquely rotated T-mode PCA can be used to enhance the understanding of the continuous nature of atmospheric circulations and the climate drivers that modulate the regional circulation patterns.

The finding that the SAM has more impact on atmospheric circulations in Africa south of the equator is also relevant when considering the variability and predictability of the East and West African monsoons. The East African monsoon system is characterized by a bimodal rainfall pattern, primarily influencing the region's climate. This pattern results in two distinct rainy seasons: the "long rains" from March to May and the "short rains" from October to December. The West African monsoon, on the other hand, exhibits a unimodal rainfall pattern, with the rainy season typically running from June to September. Moreover, though this study is focused on DJFM, earlier studies (e.g., Ibebuchi 2021c) reported statistically significant all-season correlations between the climate modes and the same CTs.

The SAM's influence on SLP in the mid-latitudes can indirectly affect the position and intensity of the inter-tropical convergence zone, which is a critical factor in the onset, duration, and cessation of both the East and West African monsoon systems. For instance, during periods when the SAM exerts a stronger influence on the regional atmospheric circulations, alterations in the mid-latitude high-pressure systems could shift the timing or intensity of the inter-tropical convergence zone, potentially affecting the onset and cessation of the long and short rains. Specifically, the SAM's role could be crucial in enhancing the understanding of the early cessation of the short rains in December when we recorded strong correlations, and how shifts in atmospheric circulation might impact the subsequent March onset window for the bimodal pattern.

Furthermore, the recent study by Roy and Troccoli (2024) investigated the combined impact of the ENSO and the Indian Ocean Dipole (IOD) on East Africa's monsoon rainfall during the October–November-December season. The study revealed that both climatic phenomena, especially when occurring in the same phase, significantly influence rainfall patterns, potentially leading to either an excess or deficit in rainfall. This dual influence highlights the importance of considering both ENSO and IOD in forecasting efforts in the region. The study aligns with and expands upon findings in existing literature, notably addressing the strong influence of the Walker circulation in modulating the East African monsoon and highlighting the potential for

improved seasonal rainfall prediction by integrating these key climate drivers.

In the case of the West African monsoon, the SAM's influence on mid-latitude atmospheric circulation could also modulate the strength and positioning of the inter-tropical convergence zone over West Africa. Although the direct linkage might be less apparent due to the primarily unimodal rainfall pattern, the underlying atmospheric dynamics influenced by the SAM could still play a role in the year-to-year variability of the monsoon onset, duration, and intensity.

4 Conclusions

This study examined the relative contributions of ENSO and the SAM in the seasonal variability of the leading regional modes of atmospheric circulation in Africa, south of the equator. The results showed that during austral summer (DJFM), the SAM is relatively more related to the leading circulation modes compared to ENSO. Specifically, the SAM explained about 20% to 46% variance of the leading circulation modes. The predictability in the inter-annual variability of the leading circulation modes using ENSO and the SAM was found to significantly improve when the co-variability between the classified CTs is considered. The broader implication of this study is that variation of the SAM is notably a source of predictability of summer atmospheric circulations over southern Africa.

Appendix 1

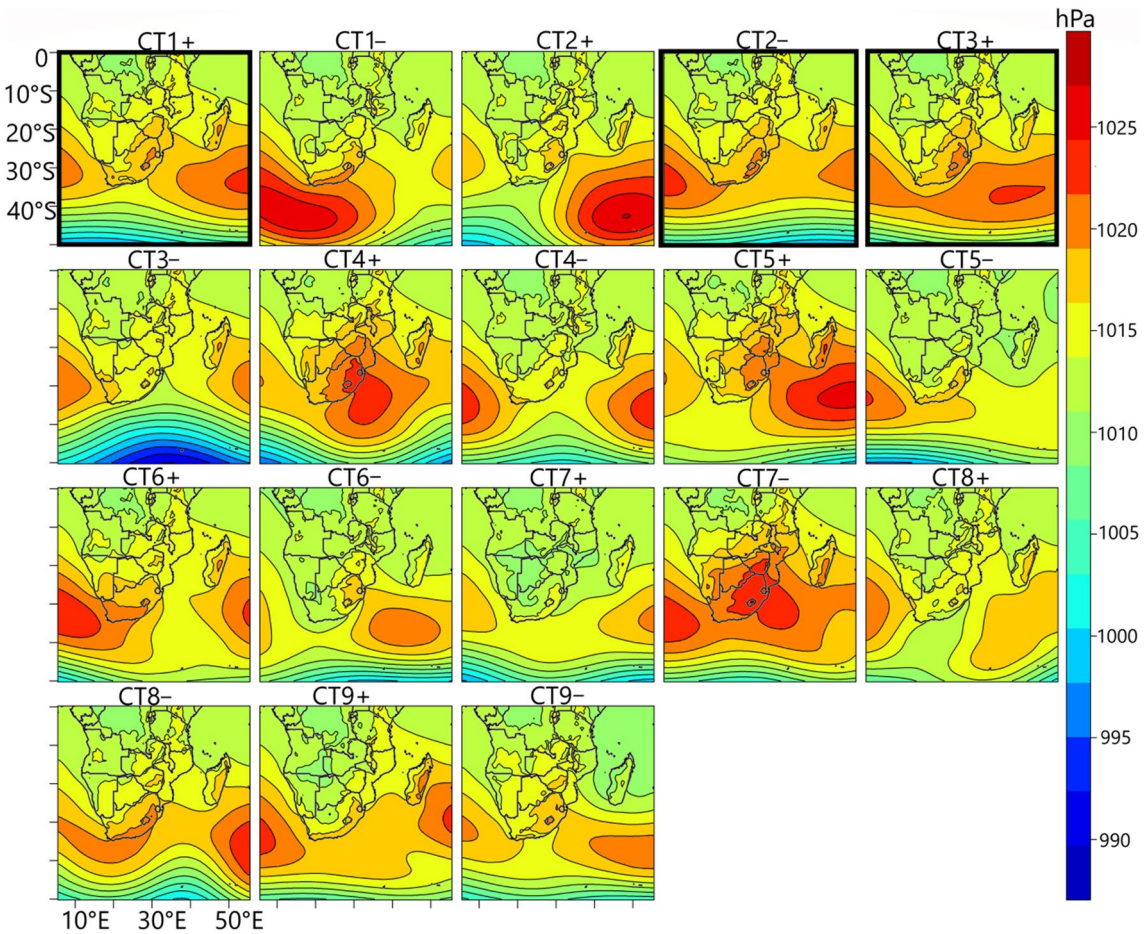

Fig. 5 Circulation types in Africa south of the equator. The circulation types with the highest probability of occurring are highlighted by the thick black frames. They are featured in the first three retained components

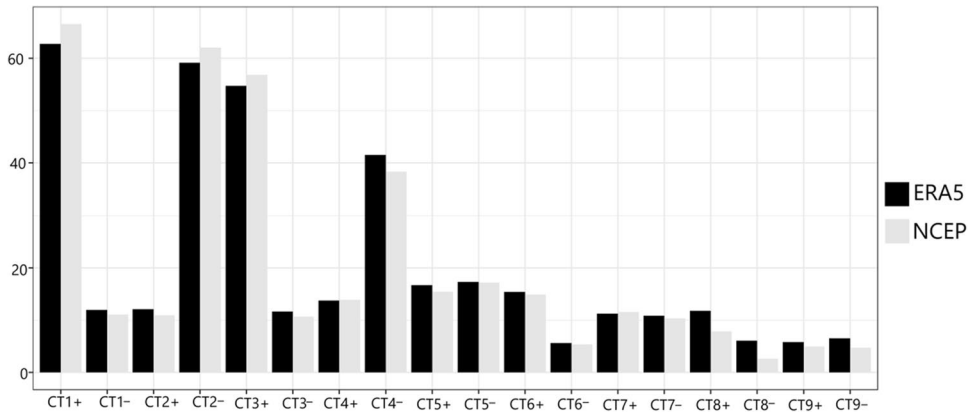

Fig. 6 The probability of occurrence of the circulation types in Fig. 5 from the NCEP and ERA5 data classifications

Appendix 2

Classification of circulation types using the obliquely rotated T-mode PCA

The classification of the CTs is completely eigenvector-based (Ibebuchi and Richman 2023; Ibebuchi and Lee 2024). It involves the application of obliquely rotated PCA to the T-mode correlation matrix of the z-score standardized SLP field. Singular value decomposition is applied to the data matrix to obtain the PC scores, eigenvalues, and eigenvectors. The PC scores capture the input spatial patterns, and the eigenvectors localize the patterns in time. To make the eigenvectors responsive to rotation they are multiplied with the square root of their corresponding eigenvalues so that they become PC loadings. The loadings are rotated obliquely using Promax at a power of 2. The oblique rotation aims to obtain a simple structure that is physically interpretable by maximizing the number of near-zero loadings. Following its efficacy, in previous studies, $\pm$ 0.2 is used in this study to separate signal from noise. Introducing the threshold allows a day can be classified under more than one PC pattern insofar as the PC pattern has signal magnitude $>|0.2|$ on that day. Each retained PC gives two asymmetric classes (i.e., clusters above or below the $\pm$ 0.2 threshold) and the SLP mean of the days in a given class is the CT.

Acknowledgements Thanks to Copernicus Climate Change Service and NOAA/OAR/ESRL PSL for providing the ERA5 and NCEP-NCAR reanalysis data sets, respectively.

Author contributions Work was designed and executed by Chibuike Ibebuchi.

Funding Dr Ibebuchi is funded as postdoctoral researcher at Kent State University through NOAA Award Number NA22OAR4310142 (PI: Dr Cameron C Lee).

Data availability The NCEP-NCAR reanalysis data sets are available at https://psl.noaa.gov/data/gridded/data.ncep.reanalysis.html. ERA5 data are available athttps://cds.climate.copernicus.eu/cdsapp#!/dataset.

Declarations

Ethics approval No human subject is involved in this study and Figures belong to the author. The paper is also not under consideration in any Journal. There is also no conflict of interest in this paper.

Consent to participate No human research is used. The author consent this paper to be considered.

Consent for publication The author consent this paper to being published.

Competing interests The authors declare no competing interests.

References

Compagnucci RH, Araneo D, Canziani PO (2001) Principal sequence pattern analysis: a new approach to classifying the evolution of atmospheric systems. Int J Climatol 21:197–217

Cook KH (2000) The South Indian convergence zone and interannual rainfall variability over Southern Africa. J Clim 13:3789–3804

Dieppois B, Rouault M, New M (2015) The impact of ENSO on southern African rainfall in CMIP5 ocean atmosphere coupled climate models. Clim Dyn 45:2425–2442

Dieppois B, Pohl B, Rouault M, New M, Lawler D, Keenlyside N (2016) Interannual to Interdecadal variability of winter and summer southern African rainfall, and their teleconnections. J Geophys Res: Atmos 121:6215–6239

Ding Q, Steig EJ, Battisti DS, Wallace JM (2012) Influence of the tropics on the Southern annular mode. J Clim 25:6330–6348

Engelbrecht CJ, Landman WA (2016) Interannual variability of seasonal rainfall over the Cape south coast of South Africa and synoptic type association. Clim Dyn 47:295–313

Hall A, Visbeck M (2002) Synchronous variability in the southern hemisphere atmosphere, sea ice, and ocean resulting from the annular mode. J Clim 15:3043–3057

Hart NCG, Washington R, Reason CJC (2018) On the likelihood of tropical-extratropical cloud bands in the South Indian Convergence Zone during ENSO events. J Clim 31:2797–2817

Hersbach H, Bell B, Berrisford P, Hirahara S, Nicolas J, Radu R, Simmons A, Abellan X, Soci C, Bechtold P et al (2020) The ERA5 global reanalysis. Q J R Meteorol Soc 146:1999–2049

Hoell A, Funk C, Magadzire T, Zinke J, Husak G (2015) El Niño-Southern Oscillation diversity and Southern Africa teleconnections during Austral Summer. Clim Dyn 45:1583–1599

Huth R, Beck C, Philipp A, Demuzere M, Ustrnul Z, Cahynová M, Kysely J, Tveito OE (2008) Classifications of atmospheric circulation patterns: recent advances and applications. Ann N Y Acad Sci 1146:105–152

Ibebuchi CC (2021a) On the relationship between circulation patterns, the Southern Annular Mode, and rainfall variability in Western Cape. Atmosphere 12(6):753

Ibebuchi CC (2021b) Circulation pattern controls of wet days and dry days in Free State, South Africa. Meteorol Atmos Phys 133(5):1469–1480

Ibebuchi CC (2021c) Revisiting the 1992 severe drought episode in South Africa: the role of El Niño in the anomalies of atmospheric circulation types in Africa south of the equator. Theor Appl Climatol 146:723–740

Ibebuchi CC, Lee CC (2024) Circulation pattern controls of summer temperature anomalies in Southern Africa. Adv Atmos Sci 41:341–354

Ibebuchi CC, Richman MB (2023) Circulation typing with fuzzy rotated T-mode principal component analysis: methodological considerations. Theor Appl Climatol 153:495–523

Jury MR (2015) Factors contributing to a decadal oscillation in South African rainfall. Theor Appl Climatol 120:227–237

Kalnay E et al (1996) The NCEP/NCAR 40-year reanalysis project. Bull Amer Meteor Soc 77:437–472

L'Heureux ML, Thompson DWJ (2006) Observed relationships between the El Niño-Southern Oscillation and the extratropical zonal-mean circulation. J Clim 19:276–287

Lyon B, Manson S (2007) The 1997–98 summer rainfall Season in Southern Africa. Part I: observations. J Clim 20:5134–5148. https://doi.org/10.1175/JCLI4225.1

Malherbe J, Landman WA, Engelbrecht FA (2014) The bi-decadal rainfall cycle, Southern Annular Mode and tropical cyclones over the Limpopo River Basin, southern Africa. Clim Dyn 42:3121–3138

Manatsa D, Mushore T, Lenouo A (2015) Improved predictability of droughts over southern Africa using the standardized precipitation evapotranspiration index and ENSO. Theor Appl Climatol 127:259–274

Mason SJ, Jury M (1997) Climatic variability and change over the southern Africa: a reflection on underlying processes. Prog Phys Geogr 21:23–50

Mason SJ, Tyson PD (2000) The occurrence and predictability of drought over southern Africa. In: Wilhite DA (ed) Drought, vol 1: a global assessment. Routledge, New York, pp 113–124

Morioka Y, Takaya K, Behera SK, Masumoto Y (2015) Local SST impacts on the summertime Mascarene high variability. J Clim 28(2):678–694

Philipp A (2009) Comparison of principal component and cluster analysis for classifying circulation pattern sequences for the European domain. Theor Appl Climatol 96:31–41

Pohl B, Fauchereau N, Richard Y, Rouault M, Reason CJC (2009) Interactions between synoptic, intraseasonal and interannual convective variability over Southern Africa. Clim Dyn 33:1033–1050

Pohl B, Dieppois B, Crétat J, Lawler D, Rouault M (2018) From synoptic to interdecadal variability in southern African rainfall: towards a unified view across timescales. J Clim 31:5845–5872

Reason CJC, Jagadheesha D (2005) A model investigation of recent ENSO impacts over southern Africa. Meteor Atmos Phys 89:181–205

Reason CJC, Allan RJ, Lindesay JA, Ansell TJ (2000) ENSO and climatic signals across the Indian Ocean basin in the global context: Part I, interannual composite patterns. Int J Climatol 20:1285–1327

Reason C, Landman W, Tennant W (2006) Seasonal to decadal prediction of southern African climate and its links with variability of the Atlantic Ocean. Bull Amer Meteor 87:941–956

Richman MB (1981) obliquely rotated Principal Components: an improved meteorological map typing technique? J Appl Meteorol 20:1145–1159

Richman MB (1986) Rotation of principal components. J Climatol 6:293–335

Rouault M, Richard Y (2005) Intensity and spatial extent of droughts in southern Africa. Geophys Res Lett 32:L15702

Roy I, Troccoli A (2024) Identifying important drivers of East African October to December rainfall season. Sci Total Environ 914:169615

Screen J, Gillett N, Stevens D, Marshall G, Roscoe H (2009) The role of eddies in the Southern Ocean temperature response to the southern annular mode. J Clim 22:806–818

Seager R, Harnik N, Kushnir Y, Robinson W, Miller J (2003) Mechanisms of hemispherically symmetric climate variability. J Clim 16:2960–2978

Thompson DWJ, Wallace JM (2000) Annular modes in the extratropical circulation. Part I: Month-to-month variability. J Clim 13:1000–1016

Xue F, Wang H, He J (2003) Interannual variability of Mascarene High and Australian High and their influence on the East Asian summer rainfall over East Asia. Chin Sci Bull 48:492–497